

See discussions, stats, and author profiles for this publication at:
<https://www.researchgate.net/publication/222859742>

Magnetic exchange cooperative effect of the bridges in μ -hydroxo and μ -acetato bridged chromium(III) dimers: A density functional theory coupling the broken-symmetry approach

ARTICLE *in* CHEMICAL PHYSICS LETTERS · OCTOBER 2002

Impact Factor: 1.9 · DOI: 10.1016/S0009-2614(02)01306-4

CITATIONS

14

READS

14

3 AUTHORS, INCLUDING:



Qinghua Ren

Shanghai University

29 PUBLICATIONS 222 CITATIONS

SEE PROFILE



Lei Zhang

The University of Warwick

107 PUBLICATIONS 767 CITATIONS

SEE PROFILE

Magnetic exchange cooperative effect of the bridges in μ -hydroxo and μ -acetato bridged chromium(III) dimers: a density functional theory coupling the broken-symmetry approach

Qinghua Ren, Zhida Chen ^{*}, Lei Zhang

Department of Chemistry, State Key Laboratory of Rare Earth Materials Chemistry and Applications, Peking University, Beijing 100871, China

Peking University – The University of Hong Kong Joint Laboratory in Rare Earth Materials and Bioinorganic Chemistry, Beijing 100871, China

Received 18 April 2002; in final form 9 August 2002

Abstract

The magnetic exchange behaviour for μ -hydroxo and μ -acetato double-bridged chromium(III) dimer is investigated based on calculations of density functional theory combined with the broken-symmetry approach. It is demonstrated that there is a magnetic exchange cooperative effect of the two bridging ligands in a double-bridged dimer systems with approximate equal coupling intensity. Meanwhile, the calculated results reveal that the deprotonation of the μ -hydroxo ligand causes a sharp increase of the magnetic exchange interaction between the chromium centers. Replacing either the μ -hydroxo bridging ligand by one water bridging ligand or the μ -acetato bridging ligands by two terminal water ligands produces a relatively reasonable model to examine the contribution on the magnetic exchange interaction of another individual bridging ligand.

© 2002 Elsevier Science B.V. All rights reserved.

1. Introduction

In recent years, bridged transition metal dimers are of great interest due to their simple structure and prototypical magnetic properties. Theoretical and experimental chemists have studied and developed many singly bridged early transition metal dimers, such as hydroxo-, oxo-, azido- and chloro-

bridged complexes of Ti(III), V(III) and Cr(III) [1–7]. More recently, a lot of doubly or triply bridged binuclear chromium(III) complexes have been reported, which have more than one type of bridging units, such as one hydroxo or oxo bridge together with one or more carboxylato or carboxylato bridges [8–10]. In connection with the magnetic properties of the multiple-bridged complexes, the effects of two or more bridging ligands have received considerable attention besides the normal effect of hydroxo or oxo single bridging unit

^{*} Corresponding author. Fax: +86-010-6275-1708.
E-mail address: zdchen@pku.edu.cn (Z. Chen).

[10–14]. It should be pointed out that in the previous report Lippard demonstrated that for dinuclear iron(III) centers bridged by a ligand oxygen atom (oxo, hydroxo, alkoxo, etc.) and at least one other bridging ligand (carboxylate, sulfate, phosphate, etc.) the anti-ferromagnetic exchange-coupling constants J are associated with half the shortest superexchange pathway between two iron(III) ions. That is called as the shortest superexchange pathway [11].

Recently Spiccia and coworkers [15] reported three μ -hydroxo and μ -acetato double-bridged binuclear chromium(III) complexes, $[(\text{tren})\text{Cr}(\mu\text{-OH})(\mu\text{-O}_2\text{CCH}_3)\text{Cr}(\text{tren})](\text{ClO}_4)_4 \cdot 4\text{H}_2\text{O}$ (1), $[(\text{trenH})\text{Cr}(\mu\text{-OH})(\mu\text{-O}_2\text{CCH}_3)_2\text{Cr}(\text{trenH})](\text{ClO}_4)_5 \cdot 6\text{H}_2\text{O}$ (2) and $[(\text{H}_2\text{O})_4\text{Cr}(\mu\text{-OH})(\mu\text{-O}_2\text{CCH}_3)\text{Cr}(\text{OH}_2)_4](\text{CH}_3)_3\text{C}_6\text{H}_2\text{SO}_3)_4 \cdot 8\text{H}_2\text{O}$ (3), where the two Cr(III) centers are weakly anti-ferromagnetically coupled with coupling constants J of -19.9 , -15.7 and -7.7 cm^{-1} for complexes (1), (2) and (3), respectively. It is interesting to note whether if the shortest superexchange pathway is available to these double-bridged binuclear chromium(III) complexes. Herein both the bridging hydroxo and bridging carboxylate ligands are a weak bridging ligand for the magnetic superexchange between the two Cr(III) centers. It is obvious that how to influence the magnetic exchange interaction by coexistence of the two bridging ligands with approximate equal coupling intensity is worth investigating.

In the present Letter, we pay more attention to the magnetic exchange cooperative interaction for the double-bridged binuclear chromium(III) complexes (3) mentioned above. The Letter is organized as follows: Section 2 is involved in computational approach, Section 3 describes the calculated models. Section 4 presents the calculated results and discussion. The conclusions are given in Section 5.

2. Computational details

All calculations in the present Letter have been performed with the density functional method (DFT) combined with the broken-symmetry approach (BS), proposed by Noodleman [16–19], which has demonstrated that calculations of the

exchange coupling constant for complex molecules have a good degree of accuracy. The exchange coupling constants J can be evaluated by calculating the energy difference between the high-spin state (E_{HS}) and the broken-symmetry state (E_{BS}) (assuming Heisenberg spin Hamiltonian is defined as $\hat{H} = -2J\hat{S}_1 \cdot \hat{S}_2$), according to the following expression [16]:

$$E_{\text{HS}} - E_{\text{BS}} = \left[-S_{\text{max}}(S_{\text{max}} + 1) + \sum_S^{S_{\text{max}}} A_1(S) \cdot S(S + 1) \right] J, \quad (1)$$

where S corresponds to the spin states of the molecules studied, $A_1(S)$ stands for squares of Clebsch–Gordan coefficients.

In the cases of the hydroxo- and acetato-bridged binuclear Cr(III) complexes, $[(\text{H}_2\text{O})_4\text{Cr}(\mu\text{-OH})(\mu\text{-O}_2\text{CCH}_3)\text{Cr}(\text{H}_2\text{O})_4](\text{CH}_3)_3\text{C}_6\text{H}_2\text{SO}_3)_4 \cdot 8\text{H}_2\text{O}$, where $S_1 = 3/2$ and $S_2 = 3/2$, the following expression is obtained:

$$E_{\text{HS}} - E_{\text{BS}} = -9J, \quad (2)$$

where positive value of the coupling constant J indicates ferromagnetic character and the negative value of J means anti-ferromagnetic behaviour. Eq. (2) is adopted in our calculations.

All the calculations have been carried out by using the Amsterdam Density Functional (ADF) package version 2.3. [20]. The local density approximation (LDA) with local exchange and correlation potentials makes use of Vosko, Wilk and Nusair (VWN) correlation functional [21]. Becke's non-local exchange correction [22] and Perdew's non-local correlation correction [23] are added in each SCF consistent cycle. We have used the IV basis sets in ADF, containing triple- ζ basis sets for all atoms and a polarization function from H to Ar atom. The frozen core (FC) approximation for the inner core electrons and relativistic effects are used. The orbitals up to 2p for Cr atom, up to 1s for O and C atoms are kept frozen. The numerical integration procedure applied for the calculations is the polyhedron method developed by Velde and coworkers [24,25]. The convergence standard of the system energy is smaller than 10^{-6} eV , reaching a precision required for the evaluation of the J values.

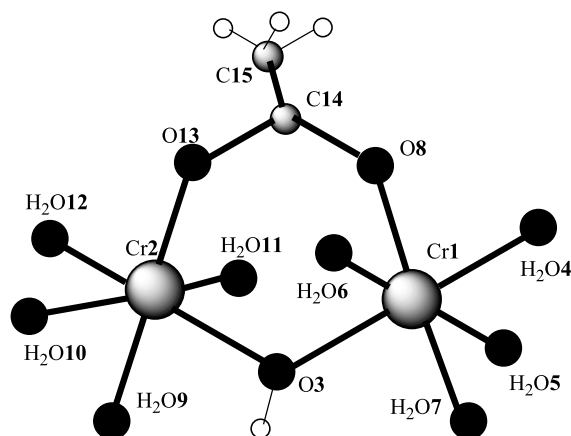


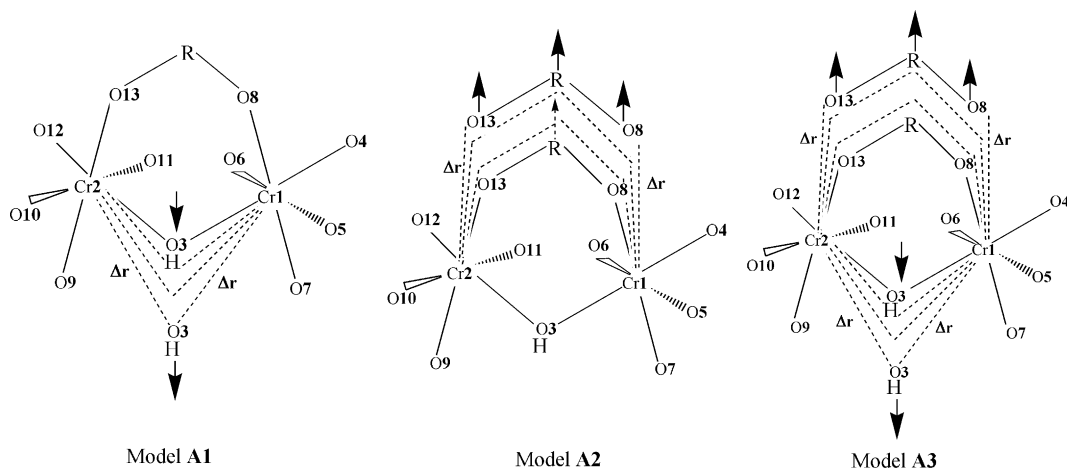
Fig. 1. The structure of model 1.

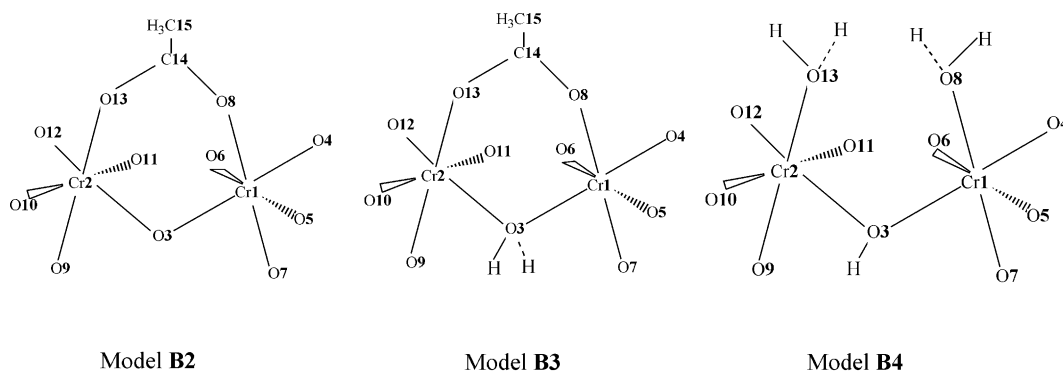
3. Calculated models

In order to investigate the magnetic exchange behaviour of the bridge ligands, we get two sets of calculated models from the complex (3), $[(\text{H}_2\text{O})_4\text{Cr}(\mu\text{-OH})(\mu\text{-O}_2\text{CCH}_3)\text{Cr}(\text{H}_2\text{O})_4][(\text{CH}_3)_3\text{C}_6\text{H}_2\text{SO}_3]_4 \cdot 8\text{H}_2\text{O}$. Fig. 1 gives a simplified view of the cation, $[(\text{H}_2\text{O})_4\text{Cr}(\mu\text{-OH})(\mu\text{-O}_2\text{CCH}_3)\text{Cr}(\text{H}_2\text{O})_4]^{4+}$, named as model 1, which is directly taken from the X-ray crystallography complete structure of this cation [15]. From the model 1, we move away the hydroxo bridging ligand from the chromium centers, illustrated as Fig. 2, to build model A1 in

order to inspect the dependence of the magnetic behaviour on the superexchange role of the bridging ligand $\mu\text{-OH}$, fixing all the other pieces of the molecule to be identical with those of model 1. Using the same method, we get another dynamic model A2 through move away of the acetato bridging ligand (cf. Fig. 2) from the chromium centers, keeping the same other factors. Model A3 is built when we move away simultaneously the two bridging ligands from the magnetic centers by the same method as mentioned above in order to examine the cooperative effect of the two bridging ligands. It should be pointed out that while the moving away the bridging ligands from the chromium centers, the $\text{Cr-O}(\mu\text{-OH}$ or $\mu\text{-O}_2\text{CCH}_3)$ distances, Δr , and Cr-O-Cr (for $\mu\text{-OH}$), Cr-O-C (for $\mu\text{-O}_2\text{CCH}_3$) angles $\Delta\theta$ are changed simultaneously. Herein we pay our attention to the superexchange role of the whole bridging ligand, otherwise detailed magneto-structural correlation. Thus the dependences of magnetic exchange behaviour on distances and angles between the bridging ligand-magnetic centers are not considered in detailed.

On the other hand, three static models are built to analyze the magnetic exchange intensity of the single hydroxo and acetato bridges in the magnetic exchange interaction. We take off the proton from the hydroxo bridging ligand to form an oxo bridging model B2, while add a proton again to the hydroxo bridging ligand to build a water

Fig. 2. The sketch maps of models A1, A2 and A3, -R denotes $-\text{C}^{14}\text{C}^{15}\text{H}_3$ group.

Fig. 3. The sketch maps of models **B2**, **B3** and **B4**.

bridging model **B3** in order to examine the single acetato bridging ligand. In addition, the model **B4** is built to analyze the exchange interaction of the single hydroxo-bridge in such way, that to take away the C–CH₃ group from the acetato bridging ligand based on the model **1**, then through double-protonation of the two remaining oxygen atoms to form two terminal water ligands which is illustrated in Fig. 3.

The purpose of all the calculations mentioned above is to explore in detail the magnetic exchange intensity of the hydroxo and acetato bridging ligands and their cooperative exchange interaction.

4. Results and discussion

4.1. Cooperative effect of two bridging ligands

The magnetic coupling constant J between the two chromium(III) centers for the species $[(\text{H}_2\text{O})_4\text{Cr}(\mu\text{-OH})(\mu\text{-O}_2\text{CCH}_3)\text{Cr}(\text{H}_2\text{O})_4]^{4+}$, model **1**, is calculated to be -10.84 cm^{-1} using DFT–BS. The experimental value reported by Spiccia and coworkers [15] is -7.7 cm^{-1} . It is indicated that the qualitative agreement between the experimental and calculated values for the coupling constant J is acceptable, shown a weak anti-ferromagnetic behaviour between the two chromium(III) centers. In this Letter, we emphasize the analysis of the dependence of the magnetic coupling constants on the specific change in the molecular structure, ignoring the small difference in

absolute value for the calculated J value compared with the experimental J value.

To examine the weak anti-ferromagnetic exchange interaction for the chromium(III) dimers, the role of the two bridging ligands is very important. We investigate herein their role based on the dynamic models (**A1**, **A2** and **A3**), and the static models (**B2**, **B3** and **B4**). In this section, we mainly present the calculated results for the dynamic models **A1**, **A2** and **A3**. And the static models **B2**, **B3**, **B4** will be investigated in next section. Model **A1** is used to examine the dependence of the magnetic coupling constant on the hydroxo bridging ligand. Because of X-ray crystallography analyses for the species **1** revealed the Cr1–O3 and Cr2–O3 to be unequal, 1.950 Å for the former and 1.918 Å for the latter, we moved the hydroxo ligand away from the Cr1 and Cr2 centers keeping the increase amount of Cr1–O3 and Cr2–O3 at a same value, Δr , in order to inspect the dependence of the magnetic coupling constants J on the increment Δr , instead of the bridge distance Cr1–O3, r_1 , or Cr2–O3, r_2 . Note that while moving away the $\mu\text{-OH}$ bridging ligand, both the Cr–O($\mu\text{-OH}$) distances r and the Cr–O($\mu\text{-OH}$)–Cr angle are changed. Herein we use the increment Δr to indicate the bridging ligand moving away. The curve A1 in Fig. 4 is a plot of $-J_1$ versus Δr when Δr varies from 0 to 0.064 Å. As shown in the curve A1, the calculated $-J_1$ values (cm^{-1}) vary with an exponential function of Δr :

$$-J_1 = 2.371 + 8.527 \exp(-44.46\Delta r), \quad (3)$$

where the correlation coefficient is 0.9984.

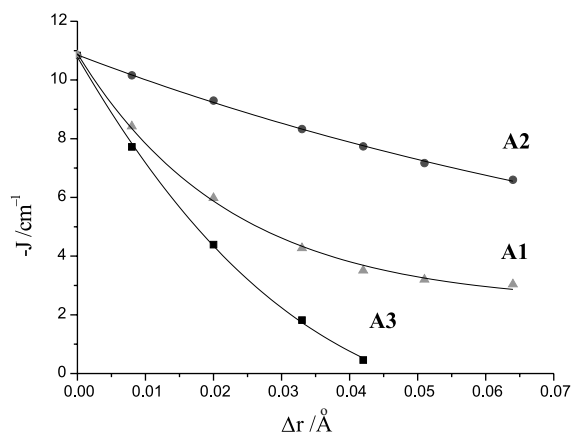


Fig. 4. The plot of exchange coupling constant J versus the variation of Cr–O distance Δr for models **A1**, **A2** and **A3**.

According to the same method to change the position of the whole acetato bridging ligand, the model **A2** is built, keeping the increments of the bridge distance Cr1–O8 and Cr2–O13 at a same value, Δr , ranging from 0 to 0.064 Å, as the model **A1**. The curve **A2** in Fig. 4 shows that the calculated $-J_2$ values (cm^{-1}) vary also with an exponential function of Δr

$$-J_2 = 1.075 + 9.781 \exp(-9.057\Delta r), \quad (4)$$

where the correlation coefficient is 0.9992.

It is evident that the curve **A1** more sharply drops as increasing Δr than in the case of the curve **A2**. This indicates that the role of the hydroxo bridging ligand in the magnetic exchange interaction is more intensity and the magnetic exchange interaction is more sensitive to the bridging ligand

moving away than in the case of the acetato bridging ligand.

When moving simultaneously the hydroxo and acetato bridging ligands (cf. model **A3**), we get the curve **A3**, the plot of $-J_3$ versus Δr , illustrated in Fig. 4. From the three curves **A1**, **A2** and **A3**, it is obvious that the decrease amount ΔJ_3 of the $-J_3$ value in the curve **A3** is approximately a summation of the changing values ΔJ_1 in curve **A1** and ΔJ_2 in curve **A2**. In order to explain this result again, we calculated the changing amount of J_1 , J_2 , J_3 value for model **A1**, **A2**, and **A3**, respectively, shown in Table 1. It is evident that ΔJ_3 indeed is approximately equal to the sum of ΔJ_1 and ΔJ_2 . All the results demonstrate a cooperative action of the hydroxo and acetato bridging ligands in moving away the two bridging ligands from the Cr(III) centers. Beyond all doubt, the cooperative action of multiple-bridges is very interesting in magnetic exchange coupling properties. It should be pointed out that both hydroxo and acetato bridging ligands are weak bridges for the chromium dimer, and their intensities in magnetic exchange interaction are approximately equivalence. Only in the condition of the equivalent bridge intensity the cooperative effect may be displayed. In the next section the intensities in the magnetic exchange interaction for these single bridges will be further examined.

4.2. Effect of single bridging ligand

In order to examine further the role of the single bridges in multiple-bridge cooperative effect, some

Table 1

Variation of the calculated magnetic coupling constant J with the increment of Cr–O, Δr^a

	Δr (Å)						
	0	0.008	0.020	0.033	0.042	0.051	0.064
J_1 (cm^{-1})	–10.84	–8.42	–5.98	–4.27	–3.51	–3.20	–3.04
J_2 (cm^{-1})	–10.84	–10.16	–9.30	–8.33	–7.74	–7.17	–6.60
J_3 (cm^{-1})	–10.84	–7.72	–4.39	–1.82	–0.46		
ΔJ_1	0	2.42	4.86	6.57	7.33	7.64	7.80
ΔJ_2	0	0.68	1.54	2.51	3.10	3.67	4.24
ΔJ_3	0	3.12	6.45	9.02	10.38		
ΔJ	0	0.02	0.05	–0.06	–0.05		

^a J_1 , J_2 , J_3 denote the calculated magnetic coupling constants for model **A1**, **A2**, **A3**, respectively; ΔJ_i stands for increase amount of J_i relative to the J value at $\Delta r = 0$; ΔJ denotes $\Delta J_3 - (\Delta J_1 + \Delta J_2)$.

models were built by replacement the individual bridging ligands with the terminal ligands, in which the models **B2** and **B3** inspect the magnetic coupling intensity of the hydroxo and acetato bridging ligands through deprotonation and protonation of the hydroxo bridging ligand. Model **B4** is through breaking down the bridging connection of the acetato bridging ligand and replacement with two terminal ligands $-\text{OH}_2$ to examine the magnetic coupling intensity of the hydroxo bridging ligand.

In our DFT-BS calculations the exchange coupling constant J values of these models are given in Table 2. A large J value (-62.01 cm^{-1}) of model **B2**, compared to the original J value (-10.84 cm^{-1}) of model **1**, is obtained. This large J value implies that the oxo bridging ligand remarkably strengthens the anti-ferromagnetic exchange interaction between the two chromium(III) centers which is in agreement with previous reports [9,10]. Furthermore, we built the water bridging ligand to replace the hydroxo bridge in model **B3**. The calculated J value is -3.66 cm^{-1} , which indicates that the water bridging ligand is weaker than the hydroxo bridging ligand. The change trend of the J values in protonation and deprotonation consists with the crucial behaviour of the hydroxo bridging ligand in the earlier report [26]. On the one hand, this indicated that the hydroxo bridging ligand indeed is a weak bridge in magnetic exchange interaction. It is well known that the water molecule is a very weak bridge in the magnetic exchange interaction between the transition metal magnetic centers. Thus, on the other hand, the J value of -3.66 cm^{-1} for model **B3** shows the main contribution of the acetato bridging ligand to the magnetic exchange interaction in a sense. This also consists with the small $|J|$ value at the larger Δr of

$\text{Cr}-\text{O}(\mu\text{-OH})$ in the curve A1 of Fig. 4, for example, J of -3.04 cm^{-1} at Δr of 0.064 \AA (cf. Table 1). It is obvious that in the case of the large Δr of $\text{Cr}-\text{O}(\mu\text{-OH})$ the magnetic exchange interaction depends mainly on the contribution from the acetato bridging ligand.

The model **B4** breaks down the acetato bridge and replaces the broken bridge with the terminal ligands in order to examine the contribution of the remained hydroxo bridge in magnetic exchange interaction. The two terminal water ligands in model **B4** are created to replace the acetato bridging ligand. The calculated J value for model **B4** is -5.89 cm^{-1} , which is approximately equal to the contribution of the single hydroxo bridging ligand. Again, we can find the consistency with the small J value, for example, J of -6.60 cm^{-1} at the larger Δr (0.064 \AA) of $\text{Cr}-\text{O}(\mu\text{-O}_2\text{CCH}_3)$ in the curve A2 of Fig. 4. On the bases of the calculated exchange coupling constants for the models **B3** and **B4**, -3.66 and -5.89 cm^{-1} , respectively, it is obvious that the single hydroxo bridging ligand has more intensity than that of the acetato bridging ligand in the magnetic exchange interaction between two Cr(III) centers. And in the whole molecule the magnetic exchange interaction is the contribution from the two bridging ligands. In the weak double-bridging system the approximate equivalent weak bridges display their cooperative effect in the magnetic exchange interaction.

4.3. Spin population analysis

In order to further explain the magnetic exchange mechanisms, the spin population analyses are used. Some mechanisms, such as the spin delocalization [27] and spin polarization mechanisms [28–30], succeeded in dealing with the binuclear systems [31]. Table 3 gives the calculated

Table 2
The calculated magnetic coupling constant J in static models

	Model			
	Model 1 ^a	Model B2	Model B3	Model B4
$J (\text{cm}^{-1})$	-10.84	-62.01	-3.66	-5.89

^a Experimental J value is -7.7 cm^{-1} .

Table 3
Spin population on the selected atoms in models **1**, **B2**, **B3** and **B4**^a

Atom	Model 1		Model B2		Model B3		Model B4	
	HS	BS	HS	BS	HS	BS	HS	BS
Cr1	3.0973	−3.0776	3.0389	−2.9355	3.0979	−3.0956	3.1314	−3.1139
Cr2	3.1036	3.0733	3.0023	2.8981	3.1190	3.1038	3.1163	3.0962
O3	−0.0333	0.0078	0.1045	−0.0388	−0.0488	−0.0017	−0.0274	0.0067
O4	−0.0272	0.0291	−0.0181	0.0221	−0.0378	0.0400	−0.0311	0.0337
O5	−0.0266	0.0273	−0.0239	0.0242	−0.0270	0.0272	−0.0286	0.0292
O6	−0.0313	0.0314	−0.0273	0.0270	−0.0342	0.0348	−0.0305	0.0302
O7	−0.0240	0.0241	−0.0210	0.0217	−0.0251	0.0248	−0.0291	0.0291
O8	−0.0012	0.0266	−0.0154	0.0396	0.0210	0.0049	−0.0232	0.0240
O9	−0.0248	−0.0251	−0.0210	−0.0216	−0.0238	−0.0240	−0.0297	−0.0296
O10	−0.0264	−0.0263	−0.0225	−0.0221	−0.0288	−0.0285	−0.0286	−0.0285
O11	−0.0252	−0.0256	−0.0221	−0.0221	−0.0261	−0.0258	−0.0261	−0.0266
O12	−0.0264	−0.0307	−0.0154	−0.0204	−0.0381	−0.0436	−0.0274	−0.0308
O13	−0.0090	−0.0283	−0.0175	−0.0379	0.0052	−0.0125	−0.0205	−0.0214
C14	0.0224	−0.0056	0.0351	−0.0051	0.0116	−0.0063		
C15	−0.0092	−0.0004	−0.0091	−0.0002	−0.0083	−0.0012		

^a Positive and negative values denote populations for α and β spins, respectively; HS and BS denote the high-spin state and the broken-symmetry state, respectively.

spin populations distribution on the central chromium(III) atoms and the peripheral atoms for the models **1**, **B2**, **B3** and **B4** in the high-spin states (HS) and the broken-symmetry state (BS), where the plus and minus signs indicate α and β spin states, respectively. Though the broken-symmetry state is a mixed spin state with $M_s = 0$, not to be a pure spin state, the state represents an averaged anti-ferromagnetic alignment of spins in a sense. It is found in Table 3 that the spin population on each chromium(III) atom is close to 3 unities while the spin populations on other atoms are very little. This point shows that the two Cr(III) centers are indeed the magnetic centers in the molecule. On the bases of the spin polarization mechanism, the spin population distributions propagate with the alternate sign away from the chromium centers to peripheral atoms in both the HS and BS unless the counteract effect due to the competition of the opposite polarization from two adjacent atoms. For model **1**, in the HS Cr1 and Cr2 have α spin population (3.0973 and 3.1036), while their peripheral atoms, for example, the bridging atoms O3(−0.0333) and O8(−0.0012) as well as terminal ligand atoms O4(−0.0272), O5(−0.0266), O6(−0.0313), O7(−0.0240) have β spin populations due to polarization from Cr(III) centers. On the other hand, in the BS Cr1(−3.0776) and

Cr2(3.0733) have opposite spin populations, leading O4(0.0291), O5(0.0273), O6(0.0314), O7(0.0241) and O8(0.0266) atoms to have α spin populations from polarization of Cr1 with the β spin population while leading O9(−0.0251), O10(−0.0263), O11(−0.0256), O12(−0.0307) and O13(−0.0283) atoms to have β spin populations from polarization of Cr2 with α spin populations. It should be pointed out that the bridging atom O3 has a little of the α spin population (0.0078) due to the polarization competition from the larger β spin population of Cr1(−3.0776) and the relatively less α population of Cr2(3.0733).

On the other hand, there are the spin delocalizations from Cr atoms to O3 in model **B2**. In the HS, Cr1 and Cr2 have α spin populations (3.0389 and 3.0023, respectively), the bridging atom O3(0.1045) has also α spin population. In the BS, Cr1(−2.9355) and Cr2(2.8981) have a delocalization competition, leading O3 to have a little belt-spin population (−0.0388). It is worth noting that in model **B4** the terminal ligands $-\text{OH}_2$ replace the broken bridging acetato ligand, however, model **B4** still reproduce characteristic of the spin population distribution on the Cr(III) centers and the peripheral atoms in model **1** by the spin polarization mechanism. According to spin population analysis for model **B4**, the spin population values

on the O8 and O13 atoms of the two terminal H₂O ligands (−0.0232 and −0.0205 in the high-spin state, respectively) have the same sign as that on the O8 and O13 atoms in model **1** (−0.0012 and −0.0090 in the high spin state, respectively). Indeed, model **B4** provides a suitable model to inspect the effect of the single hydroxo bridging ligand. In general, the spin polarization mechanism causes a weak magnetic exchange interaction. Indeed, as mentioned above, there is a small magnetic exchange constant *J* in the molecule **1** due to its polarization mechanism.

5. Conclusions

The calculations based on DFT–BS method and spin population analyses show that the anti-ferromagnetic coupling in [(H₂O)₄Cr(μ-OH)(μ-O₂CCH₃)Cr(H₂O)₄]⁴⁺ (**1**) are mainly through superexchange via the two bridging ligands. For the superexchange actions of both hydroxo and acetato bridging ligands are weak and approximately equivalent each other, the cooperative effect of the hydroxo and acetato bridging ligands in the magnetic exchange interaction is displayed in the double-bridged chromium(III) dimer. The deprotonation and protonation of the bridging hydroxo ligand, leading to the production of a bridging oxo ligand (model **B2**) and a bridging water ligand (model **B3**), respectively, cause change in the magnetic exchange interaction. Due to quite weak exchange interaction of the water bridge, the role of the acetato bridging ligand in model **B3** is displayed. Spin population analyses show that model **B4** is a suitable model for examining the action of the hydroxo bridging ligand in the magnetic exchange interaction. The calculations on model **B4** show that though the contribution of the hydroxo bridging ligand to the magnetic exchange interaction of model **1** exceeds that of the acetate bridging ligand, the superexchange actions of these weak bridging ligand are approximately equivalent. Spin population analyses also show that the polarization mechanism occurs in magnetic exchange interaction of model **1**, leading a weak spin-coupling between the two Cr(III) centers.

Acknowledgements

This project is supported by the National Nature Science Foundation of China (Grants 29831010, 20023005) and State Key Project of Fundamental Research of China (Grant G1998061305).

References

- [1] W.W. Lukens Jr., R.A. Andersen, *Inorg. Chem.* 34 (1995) 3440.
- [2] K. Fink, R. Fink, V. Staemmler, *Inorg. Chem.* 33 (1994) 6219.
- [3] R.D. Sanner, D.M. Duggan, T.C. McKenzie, R.E. Marsh, J.E. Bercaw, *J. Am. Chem. Soc.* 98 (1976) 8358.
- [4] H. Weihe, H.U. Gudel, *J. Am. Chem. Soc.* 120 (1998) 2870.
- [5] A. Bonder, P. Jeske, T. Weyhermuller, K. Wieghardt, E. Doubler, H. Schmalle, B. Nuber, *Inorg. Chem.* 31 (1992) 3737.
- [6] P. Jeske, K. Wieghardt, B. Nuber, *Inorg. Chem.* 33 (1994) 47.
- [7] S.G. Brand, N. Edelstein, C.J. Hawkins, G. Shalimoff, M.R. Snow, E.R.T. Tiekink, *Inorg. Chem.* 29 (1990) 434.
- [8] P. Andersen, H. Matsui, K.M. Nielsen, A.S. Nygaard, *Acta Chem. Scand., Ser. A* 48 (1994) 542.
- [9] L. Spiccia, G.D. Fallon, A. Markiewicz, K.S. Murray, H. Riesen, *Inorg. Chem.* 31 (1992) 1066.
- [10] T.F. Tekut, C.J. O'Connor, R.A. Holwerda, *Inorg. Chim. Acta* 214 (1993) 145.
- [11] S.M. Gorun, S.J. Lippard, *Inorg. Chem.* 30 (1991) 1625.
- [12] O. Castell, R. Caballol, *Inorg. Chem.* 38 (1999) 668.
- [13] J. Glerup, D.J. Hodgson, E. Pedersen, *Acta Chem. Scand.* A 37 (1983) 161.
- [14] D.J. Hodgson, in: R.D. Willett, et al. (Eds.), *Magneto-Structural Correlation in Exchange Coupling Systems*, Reidel, Dordrecht, 1985, p. 497.
- [15] S.J. Brudenell, S.J. Crimp, J.K.E. Higgs, B. Moubaraki, K.S. Murray, L. Spiccia, *Inorg. Chim. Acta* 247 (1996) 35.
- [16] L. Noodleman, *J. Chem. Phys.* 74 (1981) 5737.
- [17] L. Noodleman, E.J. Baerends, *J. Am. Chem. Soc.* 106 (1984) 2316.
- [18] L. Noodleman, D.A. Case, *Adv. Inorg. Chem.* 38 (1992) 423.
- [19] J. Li, L. Noodleman, D.A. Case, in: E.I. Solomon, A.B.P. Lever (Eds.), *Inorganic Electronic Structure and Spectroscopy*, vol. 1, Wiley, New York, 1999, p. 661.
- [20] Amsterdam Density Functional (ADF), Version 2.3; Scientific Computing and Modelling, Theoretical Chemistry, Vrije Universiteit: Amsterdam, The Netherlands, 1997.
- [21] S.H. Vosko, L. Wilk, M. Nusair, *Can. J. Phys.* 58 (1980) 120.
- [22] A.D. Becke, *Phys. Rev. A* 38 (1988) 3098.
- [23] J.P. Perdew, *Phys. Rev. B* 33 (1986) 8822.

- [24] P.M. Boerrigter, G.T. Velde, E.J. Baerends, *Int. J. Quant. Chem.* 33 33 (1988) 87.
- [25] G.T. Velde, E.J. Baelends, *J. Comput. Phys.* 99 99 (1992) 84.
- [26] L. Zhang, Z. Chen, *Chem. Phys. Lett.* 345 (2001) 353.
- [27] O. Kahn, *Molecular Magnetism*, VCH, New York, 1993.
- [28] H.M. McConnell, *J. Chem. Phys.* 39 (1963) 1910.
- [29] A. Izuoka, S. Murata, T. Sugawara, H. Iwamura, *J. Am. Chem. Soc.* 109 (1987) 2631.
- [30] T.A. Albright, J.K. Burdett, M. H. Whangbo, *Orbital Interactions in Chemistry*, Wiley, New York, 1985.
- [31] J. Cano, E. Ruiz, S. Alvarez, M. Verdaguer, *Comm. Inorg. Chem.* 20 (1998) 27.